

Whole-body motion retargeting using constrained smoothing and functional principle component analysis

Saori Morishima¹, Ko Ayusawa², Eiichi Yoshida² and Gentiane Venture¹

Abstract—This paper presents a novel retargeting framework for humanoid robots that allows flexible motion representation and motion synthesis with smoothing with constraints and functional principle component analysis (Functional PCA). Constrained smoothing consists in computing base functions through optimizations with constraints including mechanical limits and stability conditions. By applying Functional PCA that is a statistic method describing given motions with principal components of functions, a variety of different motions can be expressed with a small number of parameters. We apply the proposed framework to whole-body "squat" motions to reveal that those motions can practically be classified with two components. The effectiveness of the proposed method is verified by dynamic simulations and experiments with the humanoid robot HRP-4.

I. INTRODUCTION

Thanks to progress on mechanical and computational capacity, humanoid robots are expected to be used in wider applications that take advantage of their anthropomorphic shape and structure. One of the applications is to employ a humanoid robot for evaluation of assistive devices designed for human [1]. Humanoid robots can quantitatively assess the effect of the devices by measuring the motor joint torques that are difficult to be estimated from human motion. Another application is entertainment use where traditional Japanese dance motions are reproduced by a humanoid robot [2]. Those motions can be archived as a digital motion library to maintain the tradition. Since a humanoid robot has many degrees of freedom, usually more than 30, it is difficult to design such complex motions for each joint. The conventional way of motion generation is to apply inverse kinematics (IK) to compute joint angles to achieve tasks such as manipulation with end-effectors [3], [4]. However, for the above applications in which the human-like whole-body motions are important, a method called "retargeting" has often been employed that converts the captured human motions into motions executable by a humanoid [5], [6]. This conversion should be done in such a way that the motions can be performed by a humanoid by satisfying mechanical constraints and stability conditions.

The standard process of retargeting for humanoids takes two steps. The marker positions are first converted into joint angles, and then the motion is adjusted in order to meet

the mechanical constraints such as joint limits and stability conditions. Since the measured human data are discrete and fluctuated, "smoothing" is often applied by representing the joint trajectory with linear combination of base functions, for instance composed of cubic B-spline curves [7]. Then the resultant joint trajectory is adjusted to meet joint limits and also stability conditions by maintaining ZMP [8] inside the support polygon [9].

There are, nevertheless, still two issues to be solved. The first issue is that the constraints such as joint limits and stability conditions are not taken into account during the smoothing process. Modification of trajectory after smoothing may induce inconsistency with respect to the original human motions. The second problem is that the retargeted motion does not possess flexibility in the sense that it cannot be reused to generate slightly different motions. For instance, concerning squat motions we will deal with, once a human motion is transformed into a humanoid motion, it cannot be morphed to another squat motion with a different height.

In order to overcome those issues, we introduce smoothing with constraints together with functional principal component analysis (Functional PCA) [10]. The smoothing is formulated as an optimization problem to compute the combination of base functions that already satisfy the mechanical and stability constraints. The Functional PCA is an extended version of PCA that allows describing a given function with principle components that are also functions. It brings an advantage that the same set of principle components of functions can represent different motions with a reduced number of parameters changing the combinations. Moreover, different motions can be synthesized through Functional PCA, which offers even further variety of humanoid motions.

This paper is organized as follows. After surveying related works in Section II, we will present the proposed framework of motion retargeting and synthesis based on functional PCA in Section III. Section IV provides examples of the whole-body motions generated by our framework to demonstrate its smoothing and synthesis capability before summarizing the paper.

II. RELATED WORK

There are several studies about motion retargeting for a humanoid robot. Miura et al. devised a retargeting method by focusing on generating walking pattern [9]. This method allows the robot to walk similar to human by walking with stretching knee and single support phase on its toe. Moulard et al. integrated several kinematic and dynamic constraints into unified optimization problem [11]. Suleiman et al. [7]

¹S. Morishima and G. Venture are with Department of Mechanical Systems Engineering, Graduate School of Engineering, Tokyo University of Agriculture and Technology.

²K. Ayusawa and E. Yoshida are with CNRS-AIST JRL (Joint Robotics Laboratory), UMI13218/RL Intelligent Systems Research Institute, National Institute of Advanced Industrial Science and Technology (IS-AIST), Japan. {k.ayusawa, e.yoshida}@aist.go.jp

proposed the retargeting method by parameterizing the joint trajectories by cubic B-spline and formulated the motion optimization with respect to the trajectory parameters. The trajectory optimization of a humanoid robot with balancing conditions is usually computationally expensive. Since the control points of cubic B-spline only affect a piece of the whole trajectory, the sparsity of the Jacobian matrix of the trajectory with respect to the control parameters leads the reduction of the computational cost. Due to such a computational efficiency, we also utilize cubic B-spline for representing joint trajectories in a similar manner as [7]. Some retargeting methods utilize an online controllers in order to handle the possible external disturbance. Ott et al. [12] use balancing control and direct marker control in their method. The virtual markers computed from human motion by hidden Markov model generate the motion of a robot via the direct marker controller. In this paper, we utilize the motion optimization approach without controllers. On the other hand, some methods based on motion optimization are not conflicted with their work [12]; instead of hidden Markov model, the virtual markers could also be generated from the joint trajectories by forward kinematics computation.

Though the above related works are mainly dealing with the motion retargeting problem, we additionally focus on extracting the motion feature or primitive from motion trajectories in order to synthesize them. Several studies utilize multivariate PCA or similar techniques for motion classification and generation of humanoid systems. Lim et al. [13] represent the human joint trajectories by the linear combination of the basis trajectories and applied PCA to extract the bases in order to reduce the variables of motion optimization. Matsubara et al. [14] present a method for learning dynamic movement primitives from multiple set of motion trajectories. The method extracts the bases of time sequenced trajectories from those generated by a single primitive, and represents and obtains the bases with the normalized Gaussian network model. In contrast to those studies applying PCA to the time sequenced samples, Alleotti et al. [15] applied Functional PCA and classified different motions in lower dimensional functional space. The method utilized cubic B-spline as the base functions and generated representative motion of the arms. This work focused on the upper body movement. In our case, however, physical consistent conditions like balancing are additionally required. In order to utilize both the motion optimization and classification, we choose cubic B-spline curves as the base trajectory function in motion optimization, and apply Functional PCA to them in order to extract the functional bases. Our framework is featured by the additional conditions for physical consistency when synthesizing in low dimensional space obtained from Functional PCA and generating joint trajectories. The conceptual diagram of our framework is illustrated in Fig.1

III. CONSTRAINED MOTION SMOOTHING AND SYNTHESIS WITH FUNCTIONAL PCA

When we design whole-body motions of a humanoid robot, the large number of its coordinate variables makes the

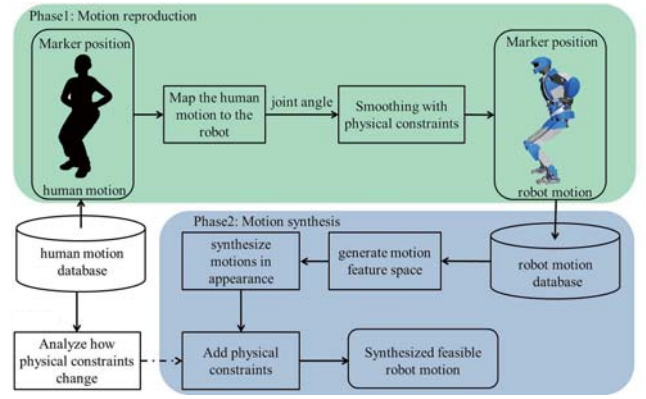


Fig. 1. Conceptual diagram of the proposed framework.

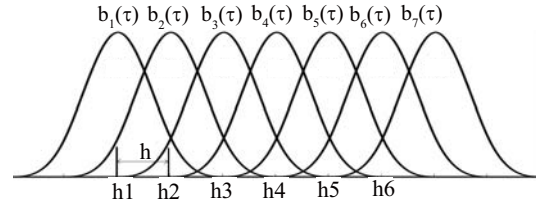


Fig. 2. Example of the base function composed of cubic B splines which have 11 nodes and 10 small sections ($m = 7$)

problem difficult. One useful approach is generating whole-body motion by fewer variables. In this paper, a smoothing technique is adopted; the trajectory of whole-body motion can be parameterized by a small set of coefficient parameters of base functional curves. At the same time, physical consistent conditions like stability have to be considered simultaneously. This section presents the retargeting method based on smoothing with considering those conditions, together with Functional PCA that allows designing whole-body motions by controlling a small set of parameters. Functional PCA can reduce the dimension of motion data-set, which makes it easier not only to classify several motions but also to extract the information about motion similarity. This section also shows the notion of motion synthesis framework by utilizing the low-dimensional space spanned by Functional PCA.

A. Smoothing with physical consistent conditions

Smoothing is a method for estimating a time curve (trajectory) fitting to a given time-series samples according to a regression model. Since the estimated curve does not need to pass exactly the points of samples, smoothing is expected to be robust to fluctuation and missing samples. Smoothing of a joint angle trajectory of a robot can be expressed according to the following regression:

$$\mathbf{q}(\tau) = \sum_{i=1}^{N_B} \mathbf{c}_i b_i(\tau) \quad (1)$$

where, $\mathbf{q}(\tau) \in \mathbb{R}^{N_j}$ is the vector of joint angles at time instant τ (bold variables mean vectors or matrices, and normal ones are scalars), N_j means the number of joints, $b_i(t) \in \mathbb{R}$ represent a cubic B spline function, N_B shows the number of

the spline functions, $\mathbf{c}_i \in \mathbb{R}^{N_j}$ is the coefficient vector. Each function $b_i(\tau)$ is aligned at regular intervals as shown in Fig.2. Let h be the interval between two spline functions. In this case, each cubic B spline function $b_i(\tau)$ can be written as follows:

$$b_i(\tau) = \begin{cases} \frac{1}{6h} \{(2-s)^3 - 4(1-s)^3\} & (0 \leq s \leq 1) \\ \frac{1}{6h} (2-s)^3 & (1 \leq s \leq 2) \\ 0 & (\text{otherwise}) \end{cases} \quad (2)$$

$$s \triangleq \frac{|\tau - h \times i|}{h} \quad (3)$$

According to the regression model, we estimate the smoothed curve from the given data samples about joint angles. Let N_T be the number of time samples, and let us redefine \mathbf{q}_t and $b_{i,t}$ as the corresponding values at time sample $t (= 1, 2, \dots, N_T)$. In this paper, we assume that time samples are given as $\tau = t \times h$.

Smoothing problem with physical consistent conditions is now formulated as the following optimization problem:

$$\begin{aligned} & \min_{\mathbf{c}_1, \dots, \mathbf{c}_{N_B}, \mathbf{r}_1, \dots, \mathbf{r}_{N_T}} \sum_{t=1}^{N_T} \|\mathbf{q}_t - \widehat{\mathbf{q}}_t\|^2 \\ & \text{subject to } \forall j, t \quad g_{j,t}(\mathbf{r}_t, \mathbf{q}_t) \leq 0 \end{aligned} \quad (4)$$

where, $\widehat{\mathbf{q}}_t$ is the given data about joint angles at time sample t , $\mathbf{r}_t \in SE(3)$ represents the position and orientation of the floating base of the robot. Problem Eq.(4) optimizes coefficient parameters \mathbf{c}_i for all base functions ($1 \leq i \leq N_B$) and floating base coordinates \mathbf{r}_t for all time samples ($1 \leq t \leq N_T$) simultaneously. Function $g_{j,t}$ ($1 \geq j \geq N_g$) means N_g set of physical consistent conditions at time sample t as followings.

a) *limitation of joint angles:*

$$\mathbf{q}_{min} \leq \mathbf{q}_t \leq \mathbf{q}_{max} \quad (5)$$

b) *geometric constraints needed for stable contacts:*

$$\mathbf{R}_{t,foot} \mathbf{e}_z = \mathbf{e}_z \quad (6)$$

$$\mathbf{e}_z^T \mathbf{p}_{t,foot} = 0 \quad (7)$$

$$\dot{\mathbf{p}}_{t,foot} = \mathbf{0} \quad (8)$$

c) *stability condition about center of mass (CoM):*

$$(\mathbf{E} - \mathbf{e}_z \mathbf{e}_z^T) \mathbf{s}_t \subset \mathbb{P} \quad (9)$$

where, \mathbf{q}_{max} and \mathbf{q}_{min} mean the boundaries of joint angles, $\mathbf{p}_{t,foot} \in \mathbb{R}^3$ ($foot = rfoot, lfoot$) is the position of the coordinate attached on the left or right foot at time sample t , $\mathbf{R}_{t,foot} \in \mathbb{R}^{3 \times 3}$ is the orientation matrix of the foot coordinates, \mathbf{e}_z is a unit vector such that $[0 \ 0 \ 1]^T$, \mathbf{s}_t is the center of total mass of the robot at time sample t , \mathbb{P} represents the motion range of the center of total mass, and the area projected on the XY plane is designed to be equal to the supporting area which is defined by the feet positions. It should be noted that Eq.(9) means static stability condition. In this paper, since we focus on several squat motions which are relatively slow, we only consider Eq.(9). In order to handle more dynamic motions, the conditions about ZMP should be considered as shown in [9].

In this paper, we solve problem Eq.(4) by the penalty function method in order to reduce the computational time for the future application like real-time retargeting. Problem Eq.(4) can be approximated as follows:

$$\min_{\mathbf{c}_1, \dots, \mathbf{c}_{N_B}, \mathbf{r}_1, \dots, \mathbf{r}_{N_T}} \sum_{t=1}^{N_T} \|\mathbf{q}_t - \widehat{\mathbf{q}}_t\|^2 + \sum_{t=1}^{N_T} \sum_{j=1}^{N_g} \lambda_j |\max(g_{j,t}, 0)|^2 \quad (10)$$

where, λ_j represents the penalty weight of each constraint $g_{j,t}$. Since the penalty function method leads the violation of constraint $g_{j,t}$, each penalty weight is usually designed according to the allowable amount of the violation. Problem Eq.(10) is solved by limited memory quasi-Newton method [16] with the fast gradient computation method [17].

B. Motion synthesis with Functional PCA

Functional PCA [10] is a statistical method for extracting important information by analyzing covariance structure and reducing dimensions of the dataset. In Functional PCA, we assume the following functional basis:

$$\boldsymbol{\xi}_t = \sum_{i=1}^{N_B} \boldsymbol{\theta}_i b_{i,t} \quad (11)$$

where, $\boldsymbol{\theta}_i \in \mathbb{R}^{N_j}$ is the vector of the parameters for regression model Eq.(11). It should be noted that same cubic B-spline functions $b_{i,t}$ are used to represent basis $\boldsymbol{\xi}_t$ and joint angles \mathbf{q}_t . Let the space spanned by the functional bases be called Functional PC space (FPC space).

We now consider the several motion dataset of joint angle trajectories; let $\mathbf{q}_t^{(n)}$ be the vector of joint angles at time sample t of n -th motion dataset, and N_M be the number of motion dataset. Regression model Eq.(1) is also reformulated as follows.

$$\mathbf{q}_t^{(n)} = \sum_{i=1}^{N_B} \mathbf{c}_i^{(n)} b_{i,t} \quad (12)$$

Let us then define the following scalar value which is called Functional PC score (FPC score):

$$f^{(n)} = \sum_{t=1}^{N_T} \boldsymbol{\xi}_t^T \mathbf{q}_t^{(n)} \quad (13)$$

The Functional PCA computes basis $\boldsymbol{\xi}$ which maximizes the variance of FPC scores as followings.

$$\text{var } f = \sum_{n=1}^{N_M} |f^{(n)}|^2 \quad (14)$$

For convenience of explanation, we concatenate parameters $\mathbf{c}_i^{(n)}$, $\boldsymbol{\theta}_i$, and $\boldsymbol{\xi}_t$, and let us define the following vectors:

$$\mathbf{c}^{(n)} = [\mathbf{c}_1^{(n)T} \ \dots \ \mathbf{c}_{N_T}^{(n)T}]^T \quad (15)$$

$$\boldsymbol{\theta} = [\boldsymbol{\theta}_1^T \ \dots \ \boldsymbol{\theta}_{N_T}^T]^T \quad (16)$$

$$\boldsymbol{\xi} = [\boldsymbol{\xi}_1^T \ \dots \ \boldsymbol{\xi}_{N_T}^T]^T \quad (17)$$

Since Eq.(14) can be transformed into the quadratic form with respect to $\boldsymbol{\theta}$, it is known that the solution can be computed by solving the following eigenvalue problem:

$$\mathbf{W} \boldsymbol{\theta}_{(k)} = \lambda_{(k)} \boldsymbol{\theta}_{(k)} \quad (18)$$

where, \mathbf{W} is the covariance matrix which can be computed from $b_{i,t}$ and $\mathbf{c}^{(n)}$ [18]. Variable $\lambda_{(k)}$ means the eigenvalue of k -th eigen vector $\boldsymbol{\theta}_{(k)}$. According to Eq.(11) and Eq.(13), we can also compute functional basis $\boldsymbol{\xi}_{(k)}$ and FPC score $f_{(k)}^{(n)}$ corresponding to k -th eigenvector $\boldsymbol{\theta}_{(k)}$.

As a result of those formulations so far, we can synthesize two motions by using the parameters space of FPC scores. Let n_1 and n_2 be the indices of motions used for synthesis. We assume the following linear combination about FPC scores:

$$\hat{f}_{(k)} = u f_{(k)}^{(n_1)} + (1-u) f_{(k)}^{(n_2)} \quad (0 \leq u \leq 1) \quad (19)$$

where, $\hat{f}_{(k)}$ means synthesized k -th FPC score.

Next, let us consider the inverse problem to reconstruct joint angle trajectory \mathbf{q} from the given set of FPC scores by using the solution of eigenvalue problem. We now define the following vector:

$$\hat{\mathbf{f}} = [\hat{f}_{(1)} \quad \cdots \quad \hat{f}_{(N_M \times N_T)}]^T \quad (20)$$

Since Eq.(13) holds for each score of $\hat{\mathbf{f}}$, by utilizing Eq.(11), Eq.(12) and the solutions of Eq.(18), we can have the following linear relationship:

$$\hat{\mathbf{f}} = \mathbf{V} \hat{\mathbf{c}} \quad (21)$$

where, \mathbf{V} is the coefficient matrix which can be computed from $\boldsymbol{\xi}_{(k)}$ and $b_{i,t}$. By solving linear form Eq.(21), we can obtain coefficient $\hat{\mathbf{c}}$ corresponding to $\hat{\mathbf{f}}$. According to Eq.(12), we reproduce joint angle trajectories $\tilde{\mathbf{q}}_t$.

Though Eq.(19) synthesizes several physically consistent motions, the synthesis process itself does not guarantee the consistent condition. In this paper, we focus on the synthesis of motions which have the same types of constraint. For example, when synthesizing the squat motion and other motions, we assume that the both feet are always contacts on ground during the motions. Then, we solve optimization problem Eq.(10) by replacing $\hat{\mathbf{q}}_t$ with $\tilde{\mathbf{q}}_t$ to realize the same constraints about physical consistency.

IV. NUMERICAL SIMULATION AND EXPERIMENT

In order to investigate the validity of the proposed retargeting framework, the optimization based on smoothing with physical constraints have been performed on a dataset of human squat motions obtained from motion capturing. The dataset includes the following three types of squat motions: the squat motion with both feet aligned, the squat with right foot in front, and with left foot in front. The retargeted squat motions were executed with both dynamic simulation Choreonoid [6] and humanoid robot HRP-4 [19]. The motion synthesis using Functional PCA have been applied to the data-set. In the Functional PCA analysis, we tested the squat motions with right or left foot in front. The several synthesized motions were created by using some set of parameter u in Eq.(19).



Fig. 3. Initial feet posture in the retargeted motions. The left and right figures show the results with and without constraint respectively.

A. Retargeting by smoothing with stability constraints

We applied the retargeting method to one squat motion which has 391 frames and the frame rate is 10 [ms]. Since the number of base functions N_B has an influence on the performance of motion reconstruction, we varied N_B and tested the method in order to experimentally find the appropriate value. Since the final cost of Eq.(10) has small change when N_B is greater than 30, we chose and fix $N_B = 30$ in the following implementations.

In order to clarify the difference of the retargeting method between with and without constraints, we at first tested the method without constraints. The obtained motions could not be performed without falling down in the dynamics simulation. When using the actual robot, HRP-4 could not realize even the initial posture of the retargeted motion. It is mainly because the foot sole planes were not horizontal as shown in Fig.3, which implies the importance of consideration about the consistent conditions.

The retargeting method by smoothing with constraints was tested on the same squat motion. Since the operation speed of the measured motion was far from the maximum speeds of the joints of the robot, we made the motions two times slower for retargeting. The squat motion obtained from motion capturing is shown in Fig.4. The snapshots of the motion simulated on the dynamic simulator are shown in Fig.5. As can be seen from Fig.5, the robot could imitate the original motion and execute the smoothed motion without violating kinematic constraints. The experimental results of smoothed squat motion with HRP-4 are shown in Fig.6. The humanoid motion was executed with a half speed of the original human motion by considering the mechanical capacity of the robot. HRP-4 could perform the motion without falling down. The simulation and experimental results verified the feasibility of the trajectory generated from constrained smoothing.

B. Motion synthesis with Functional PCA

We applied our smoothing method to the dataset consisting of two types of squat motion: the motion with the right foot in front and the other back, and the squat with the left foot in front and the other back. The dataset has 4 trials of each type of squat motion; the total number of retargeted and smoothed motion used for Functional PCA is 8. In motion synthesis process, all motions were synchronized in advance in order to have the same timing when the knee is bent. In order to have the same time duration among all motions, they were

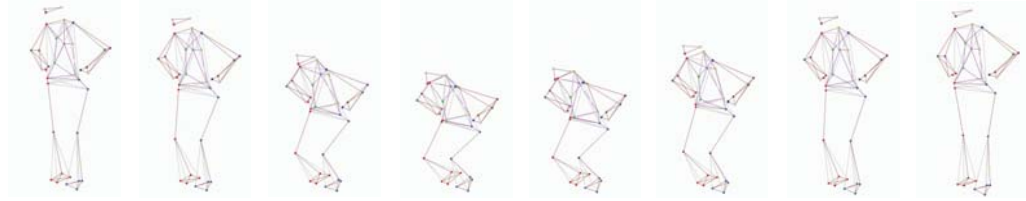


Fig. 4. Measured human squat motion

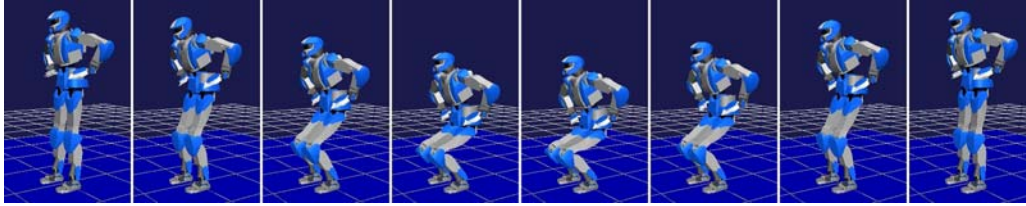


Fig. 5. Simulation result of retargeted squat motion using smoothing with stability constraints



Fig. 6. Experimental result of retargeted squat motion using smoothing with stability constraints with humanoid robot HRP-4

trimmed or extended by adding the redundant time frames before or after the motion.

All smoothed dataset were projected to the FPC space by using Eq.(13). The generated FPC space spanned by the first to third principle components is shown in Fig.7. We can recognize that the FPC scores are successfully classified according to the two types of squat motion. The red circles represent 4 samples of squat motion with left foot in front, and the green ones are those with right foot in front. Before motion synthesis, we average the FPC scores of each 4 samples. The averaged ones are illustrated as the red or green triangle in Fig.7. Let them be called the representative motions. The two types of representative motion were synthesized according to Eq.(19) with different synthesis ratio: $u = 0.3, 0.5, 0.7$ respectively. The black marks in Fig.7 show the synthesized FPC scores. The synthesized joint trajectories were computed from the synthesized FPC scores by Eq.(21). The obtained trajectory was finally modified by the smoothing process in order to realize the physical consistent conditions. Fig.8 shows the trajectories of the right ankle pitch joint during the representative motions and the synthesized motions. With the increase of the synthesis ratio, we can see that the synthesized motion becomes close to the representative squat with the left foot in front. We also tested the representative motion and the synthesized motion by using the dynamics simulation. The snapshots of the simulation results are shown in Fig.9, Fig.10, and Fig.11; Fig.9 shows the representative motion with the left foot in front, Fig.10 and Fig.11 illustrate the synthesized

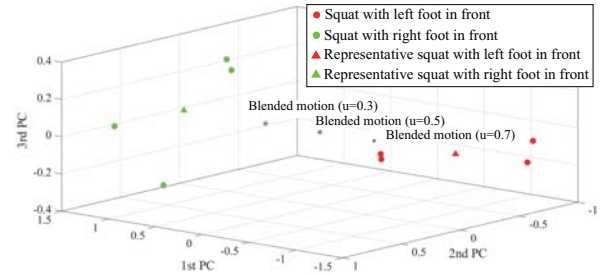


Fig. 7. FPC space spanned by two kinds of squat motion. The averaged FPC score of the two types are synthesized with different synthesis ratio.

motion with synthesis ratio $u = 0.5$ and $u = 0.3$ respectively. As can be seen from the figures, the foot placement of the robot was gradually changed according to the synthesis ratio. Especially when $u = 0.5$, the standard squat motion with the both feet aligned was generated. Those results show that various motions can be generated by synthesizing limited number of motion dataset by utilizing Functional PCA. Since the robot could perform the motion without falling down in the dynamics simulations, our framework can also guarantee the physical consistency of the synthesized motion.

V. CONCLUSION

We proposed a retargeting framework using constrained smoothing and Functional PCA with possible synthesizing of different motions. We applied this method to normal

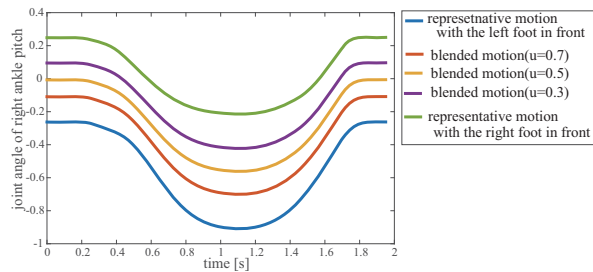


Fig. 8. Joint angle trajectories of the right ankle pitch joint in the representative motions and the synthesized motions.

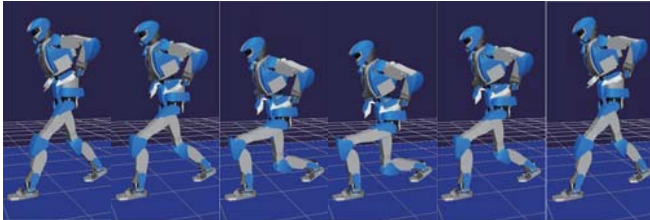


Fig. 9. Simulation result of the representative squat motion with the left foot in front

squat, squat with the right foot in front and the other back, squat with the left foot in front and the other back. All of the resulted motion succeeded in dynamic simulation and it reproduced the original human motion closely in appearance with physical constraints satisfied. The feasibility of normal squat motion was verified through the experiment with humanoid robot HRP-4. We also showed the possibility of using Functional PCA to generate various motions by synthesizing limited number of motion dataset. The several motions synthesized by our framework could be successfully performed in dynamic simulation. It indicates that our framework can guarantee the physical consistency of the synthesized motions. In our current framework, the motion synthesis and the process to add physical consistent constraints are separated. In order to synthesize the motions with several different constrains, these two processes need to be performed simultaneously, and will be addressed in our future work.

REFERENCES

- [1] K. Miura, E. Yoshida, Y. Kobayashi, Y. Endo, F. Kanehiro, K. Homma, I. Kajitani, Y. Matsumoto, and T. Tanaka, "Humanoid robot as an evaluator of assistive devices," in *Proc. of the IEEE Int. Conf. on Robotics and Automation*, 2013, pp. 671–677.
- [2] S. Nakaoka, A. Nakazawa, F. Kanehiro, K. Kaneko, M. Morisawa, H. Hirukawa, and K. Ikeuchi, "Learning from observation paradigm: Leg task models for enabling a biped humanoid robot to imitate human dances," *Int. J. of Robotic Research*, vol. 26, no. 8, pp. 829–844, 2007.
- [3] J.-J. Kuffner, K. Nishiwaki, S. Kagami, M. Inaba, and H. Inoue, "Motion planning for humanoid robots under obstacle and dynamic balance constraints," in *Proc. of the IEEE Int. Conf. on Robotics and Automation*, 2001, pp. 692–698.
- [4] E. Yoshida, O. Kanoun, C. Esteves, and J.-P. Laumond, "Task driven support polygon reshaping for humanoids," in *Proc. of the IEEE-RAS Int. Conf. on Humanoid Robots*, 2006, pp. 208–213.
- [5] K. Miura, M. Morisawa, F. Kanehiro, S. Kajita, K. Kaneko, and K. Yokoi, "Human-like walking with toe supporting for humanoids,"

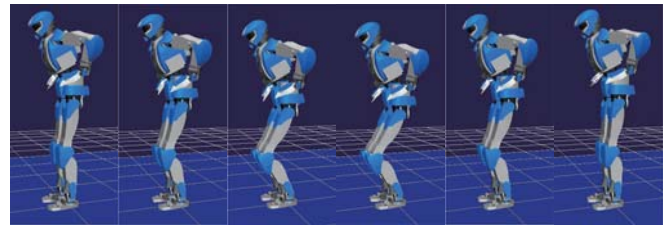


Fig. 10. Simulation result of the synthesized motion with $u = 0.5$.

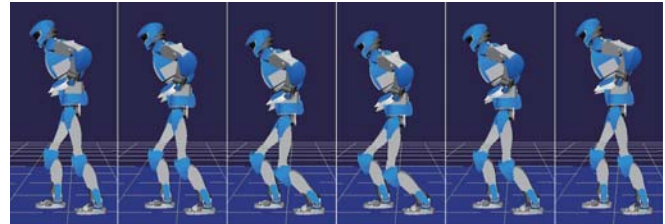


Fig. 11. Simulation result of the synthesized motion with $u = 0.3$.

- in *Proc. of the IEEE/RSJ Int. Conf. on Intelligent Robots and Systems*, 2011, pp. 4428–4435.
- [6] S. Nakaoka, "Choreonoid: Extensible virtual robot environment built on an integrated gui framework," in *Proc. of the IEEE/SICE Int. Symp. on System Integration*, 2012, pp. 79–85.
- [7] W. Suleiman, E. Yoshida, F. Kanehiro, J.-P. Laumond, and A. Monin, "Human motion imitation by humanoid robot," in *Proc. of the IEEE Int. Conf. on Robotics and Automation*, 2008, pp. 2967–2704.
- [8] M. Vukobratovic and J. Stepanenko, "On the Stability of Anthropomorphic Systems," *Mathematical Biosciences*, vol. 15, no. 1, pp. 1–37, 1972.
- [9] K. Miura, M. Morisawa, S. Nakaoka, F. Kanehiro, K. Harada, K. Kaneko, and S. Kajita, "Robot motion remix based on motion capture data towards human-like locomotion of humanoid robots," in *Proc. of the IEEE-RAS Int. Conf. on Humanoid Robots*, 2009, pp. 596–603.
- [10] P. Besse and J.-O. Ramsay, "Principal components analysis of sampled functions," *Psychometrika*, vol. 51, no. 2, pp. 285–311, 1986.
- [11] T. Moulard, E. Yoshida, and S. Nakaoka, "Optimization-based motion retargeting integrating spatial and dynamic constraints for humanoid," in *Proc. of the International Symposium on Robotics*, 2013, pp. 1–6.
- [12] C. Ott, D. Lee, and Y. Nakamura, "Motion capture based human motion recognition and imitation by direct marker control," in *Proc. of the IEEE-RAS Int. Conf. on Humanoid Robots*, 2008, pp. 399–405.
- [13] B. Lim, S. Ra, and F.-C. Park, "Movement primitives, principal component analysis, and the efficient generation of natural motions," in *Proc. of the IEEE Int. Conf. on Robotics and Automation*, 2005, pp. 4630–4635.
- [14] T. Matsubara, S. Hyon, and J. Morimoto, "Learning parametric dynamic movement primitives from multiple demonstrations," *Neural Networks*, vol. 24, pp. 493–500, 2011.
- [15] J. Aleotti and S. Caselli, "Functional principal component analysis for recognition of arm gestures and humanoid imitation," *Int. J. of Humanoid Robotics*, vol. 10, no. 4, pp. 1–25, 2013.
- [16] J. Nocedal, "Updating quasi-newton matrices with limited storage," *Mathematics of Computation*, vol. 35, no. 151, pp. 773–782, 1980.
- [17] K. Ayusawa and Y. Nakamura, "Fast inverse kinematics algorithm for large dof system with decomposed gradient computation based on recursive formulation of equilibrium," in *Proc. of the IEEE/RSJ Int. Conf. on Intelligent Robots and Systems*, 2012, pp. 3447–3452.
- [18] M. Kayano and S. Konishi, "Functional principal component analysis via regularized gaussian basis expansions and its application to unbalanced data," *J. of Statistical Planning and Inference*, vol. 139, no. 7, pp. 2388–2398, 2009.
- [19] K. Kaneko, F. Kanehiro, M. Morisawa, K. Akachi, G. Miyamori, A. Hayashi, and N. Kanehira, "Humanoid robot HRP-4 - humanoid robotics platform with lightweight and slim body," in *Proc. of the IEEE/RSJ Int. Conf. on Intelligent Robots and Systems*, 2011, pp. 4400–4407.